Investigation on the influence of concrete pores on steel corrosion process

Xiaowen Zhang, Yuxi Zhao

Institute of Structural Engineering, Zhejiang University, Hangzhou 310058, China

ABSTRACT

Concrete pores on the steel/concrete interface have a great influence on the corrosion process of steel bars. The effects of these pores on the corrosion of steel bars are observed and explored in this paper. The specimens which are in the same size and concrete proportion but have a different curing and exposure history are compared and investigated. This paper mainly observes the process of corrosion products filling into macro pores (10^{-4}-10^{-2} m in diameter) which including compaction pores (10^{-3}-10^{-2} m in diameter) and air voids (10^{-4}-10^{-3} m in diameter). These pores have different effect on the steel corrosion process, and these influences in both natural environment and artificial environment are discussed in this paper.

Keywords: Steel reinforced concrete; SEM; Corrosion; Macro pores

INTRODUCTION

As corrosion of steel bar is the leading problem causing deterioration in concrete structures (Bamforth, 2004; Cabrera, 1996; Hans, 2005; Neville, 1995; Rendell and Jauberthie, 2002), structural performance and material behavior of steel corrosion in reinforced-concrete structure has been researched by scientists and practicing engineers for decades. Corrosion in reinforced-concrete structure would cause cracking and delamination on the steel/concrete interface, and finally leads to cracking of concrete cover (Asami and Kikuchi, 2003; Duffó et al., 2004; Liu and Weyers, 1998). And then, the cracks will provide a rapid ingress path for aggressive agents to reach the reinforcement directly, which can lead to the acceleration of the corrosion process (Djerbi et al., 2008; Ohtsu and Yosimura, 1997; Wang et al., 2016; Williamson and Clark, 2000;). Since

chloride ions erosion is a main influence factor in steel corrosion, modelling for chloride-induced concrete corrosive expansion cracking has received substantial attention for researchers, and various models have been proposed (Bazant, 1979; Chernin et al., 2010; Djerbi, et al., 2008; German and Pamin, 2015; Lu et al., 2011; Ozˇbolt et al., 2014). However, in these models, the distribution of corrosion products around the steel bar has always been considered to be uniform, which obviously do not match the real chloride-induced corrosion situation (Muthulingam and Rao, 2014; Khan et al., 2014). It can be known that non-uniformly distributed corrosion products will have different effects on predicting the time to corrosion-induced cracking (Muthulingam and Rao, 2015), so it is very important to understand the non-uniform corrosion rule of steel bars in order to study the cracking model of reinforced concrete structures. In fact, the concrete pores on the steel/concrete

interface have a great influence on the corrosion process of steel bars. In this paper, the effects of these pores on the corrosion of steel bars are observed and explored.

It should be noticed that besides the accumulation around the steel/concrete interface, corrosion products will also fill into the pores in concrete, which is called the corrosion product-filled paste (CP). This paper mainly observes the process of corrosion products filling into macro pores (10^{-4}-10^{-2} m in diameter) which including compaction pores (10^{-3}-10^{-2} m in diameter) and air voids (10^{-4}-10^{-3} m in diameter). These pores have different effect on the steel corrosion process, and these influences in both natural environment and artificial environment are discussed in this paper.

EXPERIMENTAL PROBLEM

Specimens

The two specimens used in this experiment were provided by Port and Airport Research Institute in Yokosuka, Japan. These specimens are the same size and concrete proportion but have a different curing and exposure history: one specimen had been put under wetting and drying cycles to accelerate chloride ion penetration; the other was in a seawater exposure experimental facility to experience the real situation of the tidal zone of the Yokohama coastline.

The size of two concrete specimens is 100 mm × 100 mm × 150 mm, containing two 10 mm nominal diameter steel bars, as shown in Fig. 1. The nature of the mixture and the tested concrete properties are reported in Table 1.
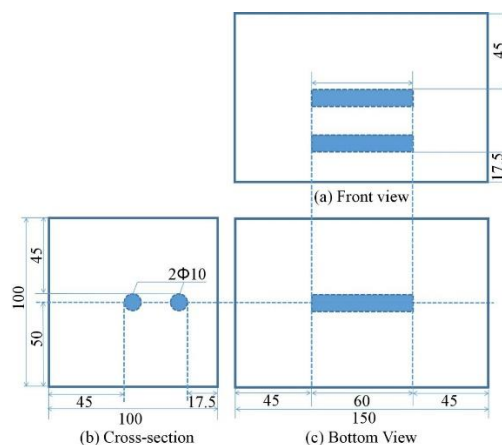
Fig. 1. Dimensions, rebar arrangement and cross-section of test piece (in mm).

Table 1. Concrete proportions of the two specimens.

| Quantities (kg/m^3)				Max size of aggregate (mm)	Air (%)	Slump (mm)	W/C
Water	Cement	Sand	Coarse aggregate				
165	243	912	970	20	4	12	0.68

The two specimens were placed, respectively, in a natural environment and an artificial environment. The specimen exposed in the natural environment is labelled N, while the other specimen in an artificial environment is labelled M.

Curing and exposure history

From October 2003 to March 2009, the specimen N was in the exposure area at the Port and Airport Research Institute to experience the real situation of the tidal zone of the Yokohama coastline. While the specimen M was in the accelerating chamber to experience wetting and drying cycles from October 2003 to March 2007 and then removed to store at room temperature. Next, both the specimens were sent to Zhejiang University in March 2009 and stored in the laboratory until unwrapped and investigated in May 2016.

Sample preparation

The specimens were cast into a low-viscosity epoxy resin to minimize artificial damage from the sample preparation process. After hardening for several days, the specimens were carefully cut to blocks by a Φ355-mm concrete cutting machine, as shown in Fig. 2. The blocks were labelled A (top) and B (bottom) according to their relative positions, with a sectional dimension of 50 mm × 50 mm. Then, the specimens were cut by a SYJ200 abrasive cutter to produce a series of 10-mm-thick cross-section slices. The slices were numbered from 1 to 5.
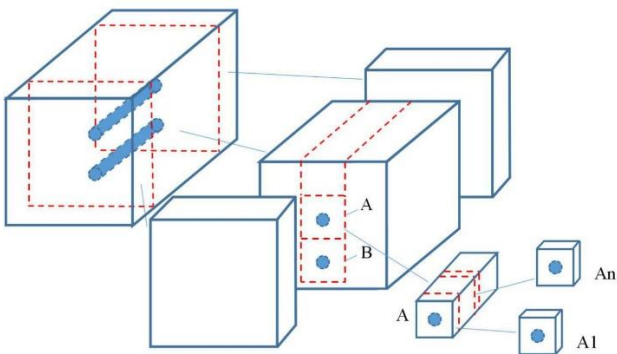

Fig. 2. Schematic diagram of the sectioned concrete blocks and the slices.

A SYJ200 abrasive cutter was used to cut slices into 25 mm × 25 mm × 8 mm samples. The samples were then polished by a UNIPOL-1502 polishing machine. After being cleaned by an ultrasonic cleaner, they were placed in vacuum-sealed bags to prevent any further corrosion.

Measurement program

The samples were observed by a scanning electron microscope (Hitachi S-3400) in the back-scattering mode. The measuring points were set at intervals of 700 μm along the perimeter of the steel bar. Approximately 30 SEM images were obtained for each sample, as shown in Fig. 3. The interface is clearly divided into five parts: steel; corrosion layer (CL); millscale; corrosion product-filled paste (CP) and concrete, as mentioned in the introduction. CL

and CP are separated by millscale which is lighter than the corrosion products. Previous studies (Cornell and Schwertmann, 1996; Zhao et al., 2013) have shown that the millscale formed before the initiation of corrosion but was not generated during the rust expansion process. The millscale does not actually contribute to the rust volume expansion acting on the surrounding concrete cover. Therefore, only CL and CP are discussed in this study. ImageJ software was used to measure T_{CL} and T_{CP}, as illustrated in Fig. 3. The thickness of CL or CP of each sample is the average value of the measurement points for each sample.
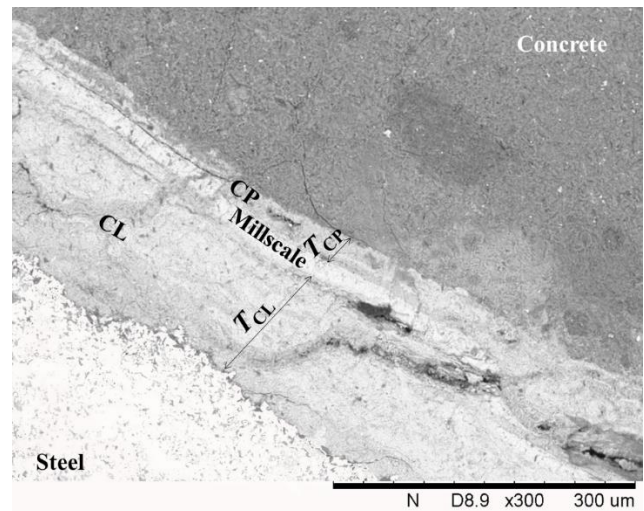

Fig. 3. Measurement of T_{CL} and T_{CP}.

The surface of the specimens was scanned by a scanner (EPSON V37) using ImageJ software to measure the width of the cracks on the concrete surface. The measuring points were set at intervals of 10 mm along the cracks. The steel-corrosion-induced crack width of the specimen is the average measured value of all of the measuring points.

INFLUENCE OF TINY CRACKS ON T_{CP}

The previous study by the authors (Zhao et al., 2014) found that there are tiny inner cracks on the interface

of steel/concrete. These tiny cracks provide a diffusion path for the corrosion products so that a large amount of corrosion products can permeate into the concrete through cracks and lead to a larger thickness of CP.

For the specimens in this experiment, a similar situation exists, in which a sudden increase of T_{CP} near the inner cracks was found in the specimen M, which experienced an artificial accelerated corrosion process, as shown in Fig. 4. Compared to the observation of the specimen in the reference (Zhao et al., 2014), which was corroded by inputting direct currents, the proportion of CP influenced by the tiny cracks in the specimen M in this study is approximately 5% of the steel bar perimeter, which is much smaller than the steel bar perimeter in the reference (Zhao et al., 2014), approximately 20%.
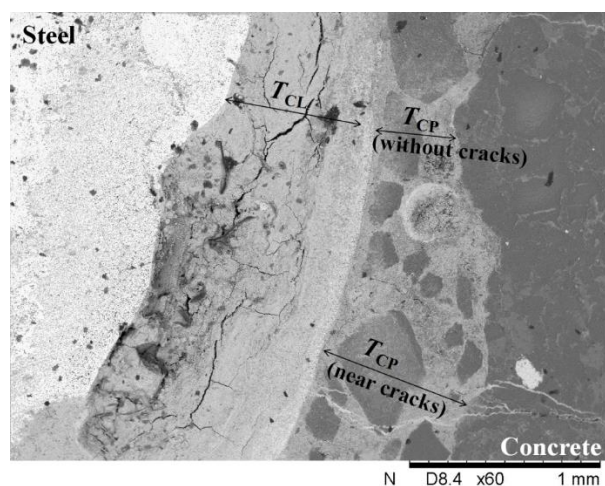
Fig. 4. The influence of tiny cracks on the value of T_{CP} (M-B5).

In previous research, the authors stated that the tiny cracks were due to the steel corrosion process accelerated by DC power. The expansion stress induced by the corrosion products could not effectively be released in a short time. Therefore, the tiny inner cracks were generated. From the observation of this experiment, it can be seen that even with wetting and drying cycles without using DC power to accelerate steel corrosion, the tiny cracks

still appear, but not as many as the situation that currents are input by DC power. Therefore, it can be inferred that the faster the steel corrosion rate is, the more tiny cracks will be generated. Because the corrosion rate accelerated by wetting and drying cycles is slower than the corrosion rate resulting from the use of DC power, the tiny cracks are also less.

In this experiment, the specimen in the natural environment, namely, the specimen N, was not observed to have any tiny cracks around the steel/concrete interface. Therefore，it can be inferred that these tiny cracks generate only when the concrete specimens have suffered from artificial accelerated corrosion, which generally much faster than nature corrosion.

Therefore, the reliability of the results obtained from the artificial steel corrosion acceleration methods, no matter by DC power or even by wetting and drying cycles, is questioned. We must use caution in using these experimental results to predict the performance of the real structures.

CORROSION PRODUCTS FILLED INTO AIR VOIDS

Because the W/C ratio of the specimen in this experiment is high, quite a few air voids were observed at the steel/concrete interface. The corrosion products filled into these air voids, as presented in Fig. 5. This phenomenon appeared in both specimens in this study.
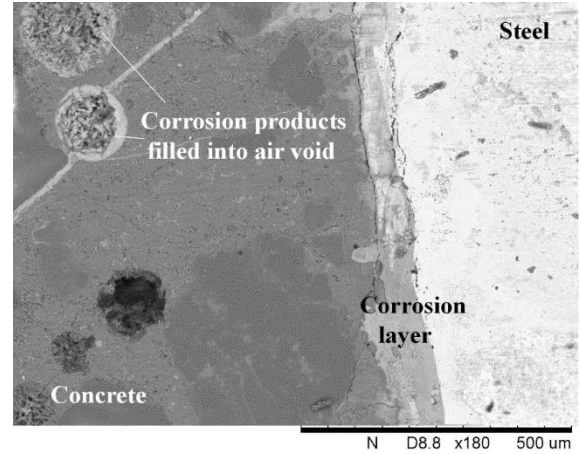
(a) M-A4

(a) M-A5

(b) N-A2

(b) N-A2

Fig. 6. Corrosion products filled into an air void (with cracks).
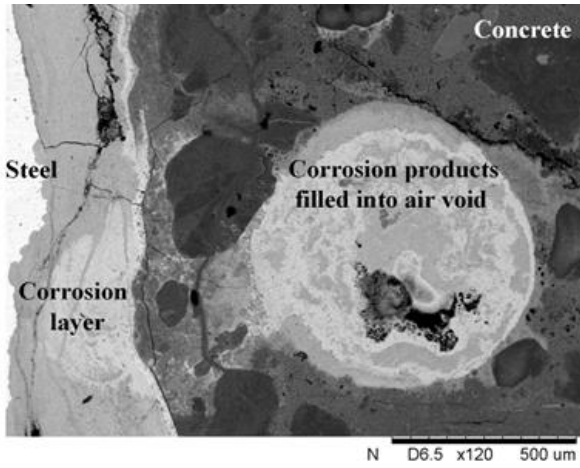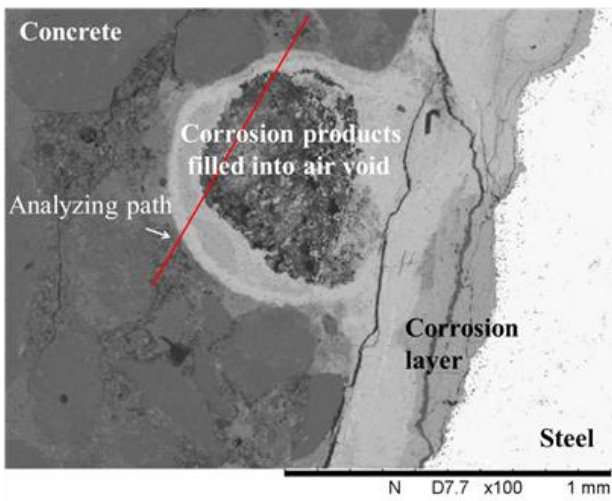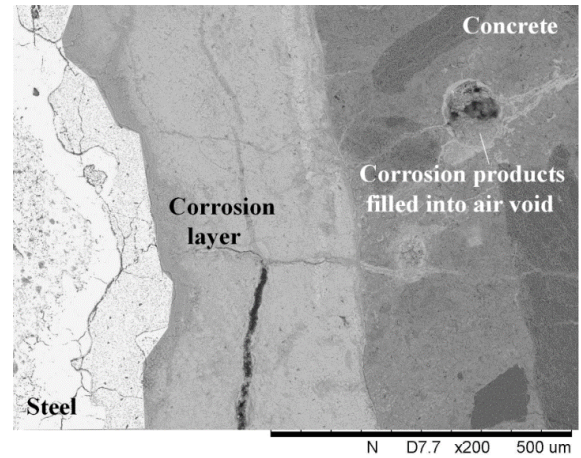
Fig. 5. Corrosion products filled into an air void.

Even considering the air voids that are not close to the steel/concrete interface, as long as there are cracks to connect the air voids and the corrosion layers, the corrosion products can also fill into air voids, as shown in Fig. 6. The air voids on the lower left corner of Fig. 6 (a) are not connected with the steel/concrete interface, so that they were not filled by corrosion products.

To analyse the component of the products filling in the air voids, the concrete pore in the sample N-A2 was examined using EDX spectroscopy. The analysis path has been shown in Fig. 5 (b), and the result is shown in Fig. 7, respectively.
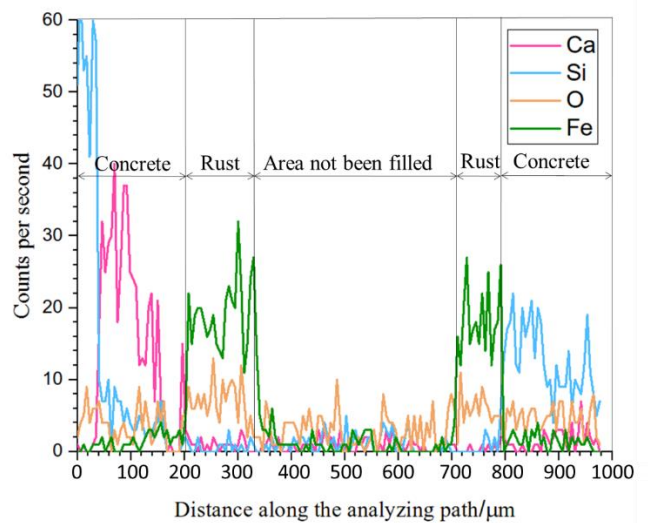

Fig. 7. Components analysis of corrosion products in the air void using EDX spectroscopy (N-A2).

Fig. 7 shows that at boundary of the pore, Fe content increases significantly, while the Ca and Si content is reduced to nearly 0, revealing that the products filling in the air voids are the same as in the corrosion layer. The dark part of the pore under analysis has not yet been filled by corrosion products, which can be observed from the EDX results in Fig. 7. This observation indicates that the corrosion products are gradually filling into the pores when the corrosion layer is thickening. This situation of corrosion products filling into the pores also has been observed in the other samples from the specimen M.

Because the cracks in the specimens in this experiment have already penetrated the concrete cover, there are many air voids still in the process of being filled according to the SEM observation. This observation proves that the penetration of corrosion products into the porous zone of concrete and the formation of a CL at the steel/concrete interface proceed simultaneously, a point which was raised previously by the authors.

In this study, many corrosion products are found filled into the air voids. Therefore, the exploration of corrosion product-filled paste should carefully consider the contribution of the quantity of corrosion products filled into the air voids, particularly if the W/C of the concrete mixture is high, similar to the concrete specimens discussed in this study.
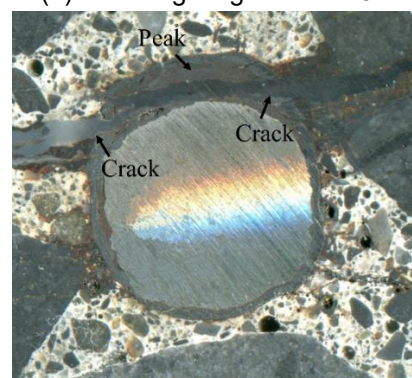
IMPACT OF MACRO PORES

The scanning diagram of the slices which have macro pores on the steel/concrete interface are observed and compared with those slices that has no pores (taking M-5-2 as an example), as shown below in Fig 8.
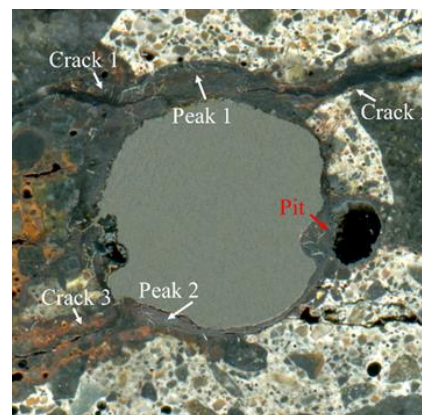
(a) scanning diagram of M-2-2
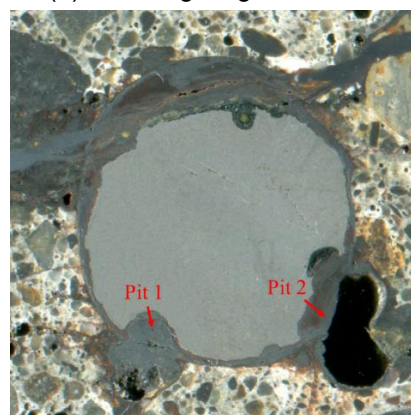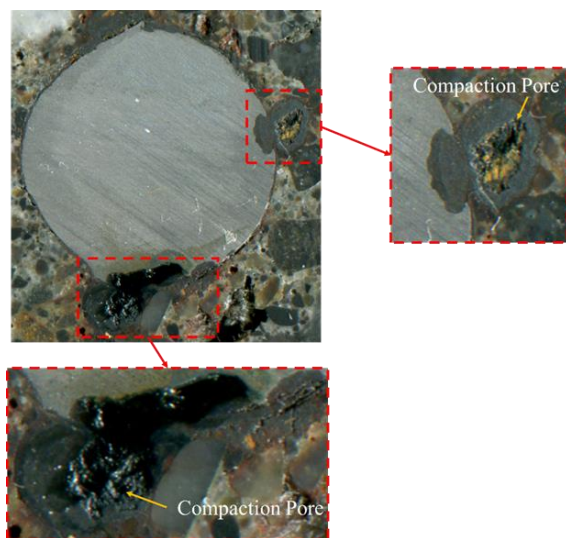

(b) scanning diagram of M-5-1

(c) scanning diagram of M-5-2

Fig.8. Comparison of steel corrosion condition of slices.

The corrosion pits which red arrows point to in Fig.8 (a) and (b) correspond to the sudden increase of the thickness of the corrosion layer. It can be seen that these corrosion pits are located in the location of compaction pore (10^{-3} -10^{-2} m in diameter) on the steel/concrete interface. While for slices which do not have macro pores on the interface, take slice M-5-2 as an example, the thickness of the corrosion layer

does not appear to increase sharply. It can be inferred that the existence of the compaction pore on the interface leads to the serious accumulation of the corrosion product in the region that does not conform to the normal law.

This situation can also be seen in the specimen which experienced natural corrosion. The following is the scanning diagram of slice N-4-2:

Fig. 9. Scanning diagram of slice N-4-2.

It can be seen that steels in natural corroded specimen are just in the primary stage of corrosion, and its corrosion layer is much thinner when compared with specimen M which has experienced artificially accelerated corrosion. But as shown in Fig. 9, the compaction pores appearing on the steel/concrete interface have been almost filled with the corrosion product, and the thickness of the corrosion layer at the pores is much larger than the rest. According to the above, the steep rise in the thickness of the corrosion layer occurs at the beginning of the corrosion process.

As the specimens are in the alternating dry and wet environment, the pores with larger diameter (10^{-4}-10^{-2} m) in diameter) centrally store water and oxygen which drive the surrounding steel to accelerate corrosion. Therefore, the corrosive process at the macro pores on the interface is independent from the development of the accumulated corrosion layer and needs to be considered separately.

According to the above observation, macro pores may be the main reason for "pitting corrosion", and "pitting corrosion" is not a necessary condition for non-uniform steel corrosion in Chloride ingress environment. Especially in natural environment, since the corrosion rate is slow, the impact of macro pores on the steel corrosion is even obvious. It can be speculated that the "pitting corrosion" situation should be reduced when the quality of the concrete is raised, such as take a series of measures to reduce the porosity of concrete which result in drastically reducing or even disappearance of the compaction pore.

CONCLUSION

The two specimens in same concrete mixture but subjecting to different environments are investigated in this study. Summarizing the corrosion condition of the test slices under different environments, it can be concluded that:

1. The specimen corroded in natural environment will not generate tiny cracks at steel/concrete interface. The tiny cracks can only be found in the specimens under artificial corroded environment which will influence the filling rate of corrosion products.

2. Quite a few corrosion products are found filled into the air void under SEM observation. The generalized CP should consider the corrosion products filled in the air void as well as the other types of pores.

3. The pores with larger diameter (10^{-4}-10^{-2} m in diameter) on the steel/concrete interface will cause the corrosion process to occur more easily and quickly.

References

Asami, K., Kikuchi, M., 2003. In-depth distribution of rusts on a plain carbon steel and weathering steels exposed to coastal - industrial atmosphere for 17 years. Corrosion Science, 45:2671 - 2688.

Bamforth, P.B., 2004. Enhancing reinforced concrete durability Guidance on selecting measures for minimizing the risk of corrosion of reinforcement in concrete. Concrete society technical report.

Bazant, Z.P., 1979. Physical model for steel corrosion in sea structures applications, Journal Of Structural Engineering-ASCE, 105 (6):1155–1166.

Cabrera, J.G., 1996. Deterioration of concrete due to reinforcement steel corrosion. Cement and Concrete Composites, 18 (1):47–59

Chernin, L., Val, D.V., Volokh, K.Y., 2010. Analytical modeling of concrete cover cracking caused by corrosion of reinforcement, Materials and Structures, 43: 543–556.

Cornell, R.M., Schwertmann, U., 1996. The Iron Oxides. Weinhaim: VHC Verlagsgesellschaft.

Djerbi, A., Bonnet, S., Khelidj, A., 2008. Influence of traversing crack on chloride diffusion into concrete, Cement and Concrete Research, 38 (6): 877–883.

Duffó, G.S., Morris, W., Raspini, I., Saragovi, C., 2004. A study of steel rebars embedded in concrete during 65 years. Corrosion Science, 46: 2143 – 2157

German, M., Pamin, J., 2015. FEM simulations of cracking in RC beams due to corrosion progress, Archives of Civil and Mechanical Engineering, 15 (4): 1160–1172.

Hans, B., 2005. Corrosion in Reinforced Concrete Structures. England: Woodhead Publishing Limited.

Khan, I., Francois, R., Castel, A., 2014. Prediction of reinforcement corrosion using corrosion induced cracks width in corroded reinforced concrete beams, Cement and Concrete Research, 56: 84–96.

Liu, Y.P., Weyers, R.E., 1998. Modeling the time-to-corrosion cracking in chloride contaminated reinforced concrete structures, ACI Materials Journal, 95: 675 - 681.

Lu, C.H., Jin, W.L., Liu, R.G., 2011. Reinforcement corrosion-induced cover cracking and its time prediction for reinforced concrete structures, Corrosion Science, 53: 1337–1347.

Muthulingam, S., Rao, B., 2015. Non-uniform corrosion states of rebar in concrete under chloride environment, Corrosion Science, 93: 267–282.

Muthulingam, S., Rao, B.N., 2014. Non-uniform time-to corrosion initiation in steel reinforced concrete under chloride environment, Corrosion Science, 82: 304–315.

Neville, A., 1995. Properties of Concrete, Longman and John Wiley, London and New York.

Ohtsu, M., Yosimura, S., 1997. Analysis of crack propagation and crack initiation due to corrosion of reinforcement, Construction and Building Materials, 11: 437–442.

Ozˇbolt, J., Orsanic, F., Balabanic, G., 2014. Modeling pull-out resistance of corroded reinforcement in concrete: coupled three-dimensional finite element model, Cement and Concrete Composites, 46: 41–55.

Rendell, F., Jauberthie, R., Grantham, M., 2002. Deteriorated concrete: inspection and physicochemical analysis. Thomas Telford Ltd.

Wang, H., Dai, J., Sun, X., 2016. Characteristics of concrete cracks and their influence on chloride penetration, Construction and Building Materials, 107:216–225.

Williamson, S.J., Clark, L.A., 2000. Pressure required to cause cover cracking of concrete due to reinforcement corrosion, Magazine of Concrete Research, 52: 455–467.

Zhao, Y.X., Ding, H.J., Jin, W.L., 2014. Development of the corrosion-filled paste and corrosion layer at the steel/concrete interface, Corrosion Science, 87: 199–210.

Zhao, Y.X., Wu, Y.Y., Jin, W.L., 2013. Distribution of millscale on corroded steel bars and penetration of steel corrosion products in concrete, Corrosion Science, 66: 160–168.

Copyright